DIFFERENTIAL THERMAL ANALYSIS CURVES OF CARBONATE MINERALS*

CARL W. BECK, *University of New Mexico, Albuquerque, New Mexico.*

ABSTRACT

Fifty-one differential thermal analysis curves are presented and interpreted. These curves are of forty-eight carbonate minerals, one artificial carbonate, one oxide mineral, and one artificial oxide.

INTRODUCTION

Differential thermal analysis studies were made on forty-eight carbonate minerals, one artificial carbonate, one oxide mineral, and one artificial oxide. The differential thermal analysis curves resulting from these studies are shown in Figs. 1–9. The discussion of the carbonates will follow the proposed classification to be used in Volume 2 of the 7th edition of Dana's *System of Mineralogy* now in preparation at Harvard University. A description of the apparatus used in the present study has been given in an earlier publication (Beck, 1950).

Usually the compounds were heated from room temperature to 1000° C. When this gave a curve that was difficult to interpret because of more than one reaction phase, additional runs were made on the original compounds. These additional runs were stopped at appropriate intermediate reaction phases as indicated by the thermal peaks. Optical and powder x-ray studies were made on these phases to aid in the interpretation of the thermal curves.

Chemical analyses were made on some of the minerals, but for the most part the identification of the minerals was established by optical and x-ray data. The chemical analyses appear in Table 7.

The numbers in parentheses after mineral names represent the minerals in the Harvard collection from which the samples were taken.

The abbreviation "DTA" should be read "differential thermal analysis."

The temperatures are in degrees Centigrade.

PROCEDURE

The heating portion of the apparatus used by the author is modelled after that of Berkelhamer (1945). The recording portion of the apparatus

* Abridged from a Ph.D. thesis, "An Improved Method of Differential Thermal Analysis and Its Use in the study of Natural Carbonates", Harvard University, 1946. Contribution from the Department of Mineralogy and Petrography, Harvard University No. 322.

is an Esterline-Angus Graphic Ammeter, appropriately amplified. Briefly, the basic principle of the amplifier is: the direct voltage generated in the thermocouple by a thermal reaction is changed to alternating voltage; the alternating voltage is then amplified to a desired amount; and, finally, the amplified alternating voltage is rectified to direct voltage in order to operate the Esterline-Angus recorder. The amplifier has a selector switch designed to pick off five different portions of the output voltage to give sensitivity Scales 1, 2, 3, 4, and 5. A comparison of the sensitivity of the different scales is shown in Table 1. The thermal changes are recorded equally well by the pen and ink recorder as by the more conventional photographic method. In addition, the author believes the pen and ink recorder, because of continual visual observation of the curve, is superior in the precision with which a thermal run may be stopped at any desired phase. The author's method of making a differential thermal analysis run is comparable to that used by other investigators.

TABLE 1. COMPARISON OF THE SENSITIVITY OF THE DIFFERENT SCALES OF THE NON-PHOTOGRAPHIC RECORDER

Scale	Average value of ΔT for 1 cm. deflection, °C.
1	4.1
2	2.4
3	0.85
4	0.21
5	0.10

EXPERIMENTAL RESULTS

Acid Carbonates

The differential thermal analysis curves of the acid carbonates are shown in Fig. 1.

Nahcolite, $HNaCO_3$ (92481) ($\alpha=1.380$, $\beta=1.500$, $\gamma=1.585$). The specimen is from Searles Lake, California. The DTA curve shows an endothermic reaction beginning at 135°, reaching a peak at 205°, and ending at 225°. The endothermic reaction is the loss of H_2O and CO_2.

The small peak at 630° is due to an admixture of magnesite. The area under this curve corresponds to 5.55% magnesite. A quantitative analysis by the author for magnesium shows 6.71% magnesite. The random deflections around 750° are due to fusing of the Na_2CO_3 at a temperature lower than the recorded fusing point of Na_2CO_3, namely 851° (Handbook of Chemistry and Physics).

Trona, $HNaCO_3 \cdot Na_2CO_3 \cdot 2H_2O$ (84568) ($\alpha = 1.414$, $\beta = 1.495$, $\gamma = 1.541$). The specimen is from an unknown locality. The DTA curve shows an endothermic reaction beginning at slightly below 100°, reaching a peak at 170°, and ending at 185°. The decomposition product is Na_2CO_3, hygroscopic in nature. The break in the curve is due to the loss of the two molecules of water of crystallization and the decomposition of the acid sodium carbonate part of the trona structure. The latter decomposition reaches

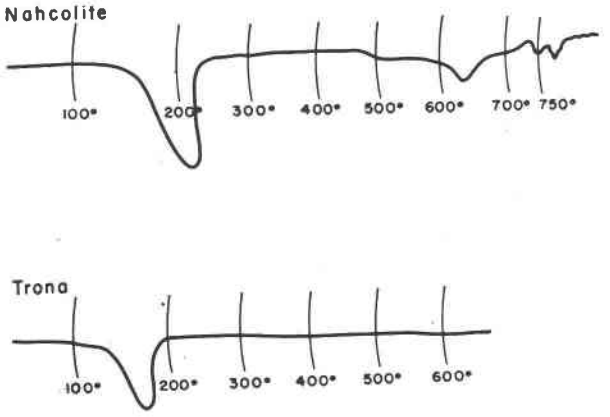

FIG. 1. Differential thermal analysis curves of the acid carbonates.

a peak at a lower temperature than the nahcolite decomposition. Two factors contribute to this: (1) the loss of the water of crystallization partially destroys the compound, increases the surface area, and makes further thermal decomposition easier; and (2) the acid carbonate makes up only 37.2% by weight of the trona structure.

TABLE 2. CHARACTERISTIC THERMAL PEAKS AND AREAS OF THE ACID CARBONATES

Mineral	Reaction product	Peak temperature, ° C.	Area, mm.²	Weight, gm.	Scale
Nahcolite	H_2O, CO_2	205	400	0.330	2
Trona	H_2O, CO_2	170	195	0.250	3

Anhydrous Normal Carbonates

I. *Calcite Group.*

A. Calcite series. The DTA curves of the calcite series are shown in Fig. 2.

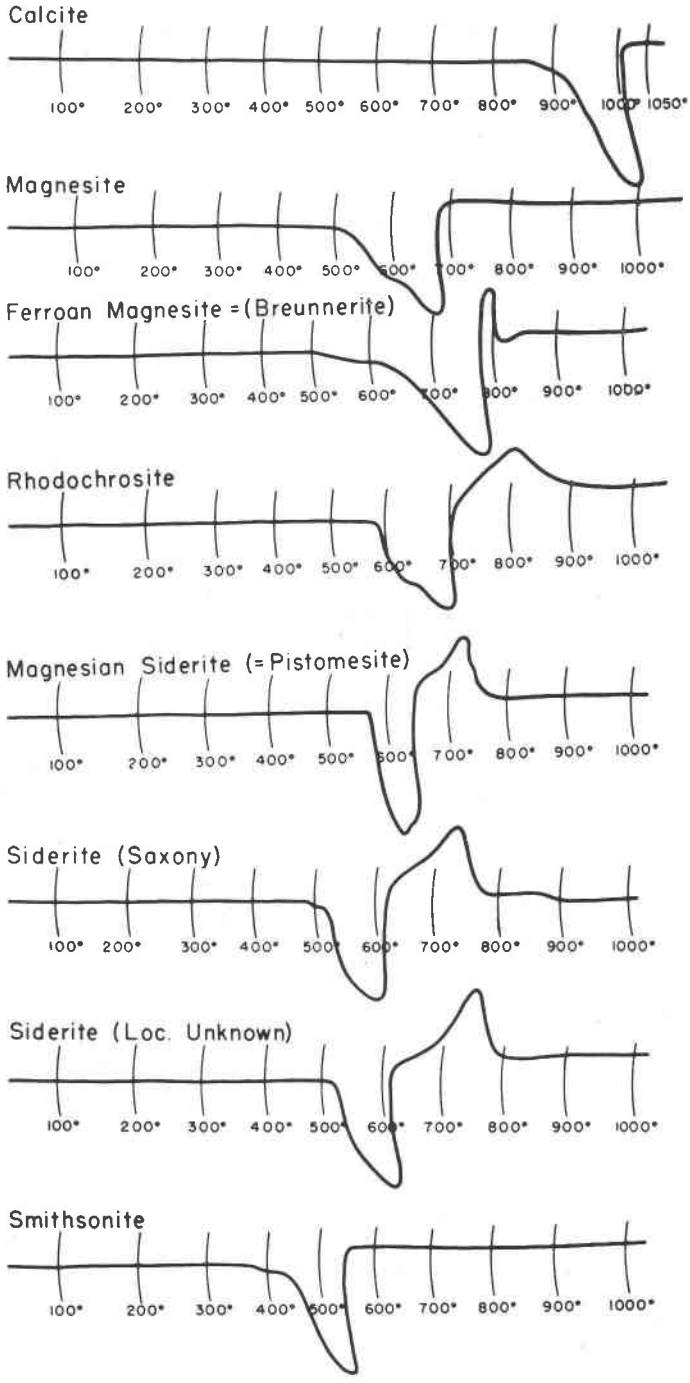

FIG. 2. Differential thermal analysis curves of the calcite series.

1. Calcite, $CaCO_3$, ($\omega = 1.658$, $\epsilon = 1.486$). The specimen is from Canada, a clear cleavage fragment of Iceland Spar. The endothermic decomposition begins at 850°, reaches a peak at 990°, and ends rapidly at 1005°.
2. Magnesite, $MgCO_3$ ($\omega = 1.703$, $\epsilon = 1.511$). The specimen is from Styria, Austria. The decomposition begins slowly at 470°, reaches a peak at 660°, and ends rapidly at 685°. The curve flattens out from approximately 570° to 600°, then the slope increases to the peak at 660°. Brill (1905) studied the dissociation of artificial normal magnesium carbonate and reported a series of small breaks corresponding to many intermediate magnesium oxy-carbonates, and one large break corresponding to $MgO \cdot MgCO_3$. Davis (1906) and Friedrich and Smith (1912) dispute the findings of Brill because neither of their investigations revealed any discontinuities in the decomposition of artificial normal magnesium carbonate. Similarly, Šplíchal, Škramovský, and Goll (1936) detected no oxy-carbonates during the decomposition of magnesium carbonate. In an effort to determine if the change in slope of the DTA curve of magnesite is due to the formation of an intermediate oxy-carbonate, optical and powder *x*-ray studies were made on the starting magnesite, on the decomposition product formed when magnesite is heated to 1000°, and on the decomposition product formed when magnesite is heated to 575°. The 1000° product is periclase, $n = 1.736$. The 575° product gives the same *x*-ray lines as the starting magnesite but the spacings are slightly different. This difference becomes greater with smaller *d's*. Optically the grains are cloudy due to decomposition; they are composed of a very fine-grained aggregate so that a grain does not show extinction between crossed nicols. The average n = about 1.72. The evidence for the formation of an intermediate oxy-carbonate is, therefore, inconclusive.
3. Ferroan Magnesite (= breunnerite), $(Mg, Fe)CO_3$, ($\omega = 1.726$, $\epsilon = 1.528$). The specimen is from Gustine, Stanislaus County, California. The chemical analysis shows 15.31% $FeCO_3$ (Table 7). The decomposition is slow from 500° to 590°, then proceeds more rapidly to the peak at 755°, and overlaps the exothermic peak representing the oxidation of ferrous oxide to ferric oxide. The latter reaches a peak at 785°. The area of the exothermic peak corresponds to 19.3% $FeCO_3$ (compare siderite), a good check with the chemical analysis. Powder

x-ray pictures show the breunnerite has the spacing of magnesite, and the decomposition product has the spacing of periclase.

4. Rhodochrosite, $MnCO_3$. The specimen is from Butte, Montana. The decomposition begins rapidly at 580°, proceeds more slowly from 615° to 625°, reaches a peak at 680°, and immediately overlaps the exothermic peak representing the oxidation of the decomposition product to Mn_3O_4. The exothermic peak is at 795°. Mn_3O_4 is the stable oxide of manganese at elevated temperatures (Pavlovitch, 1935; Mellor, Vol. XII). The curve in the region of 580–680° is probably the resultant of the decomposition of $MnCO_3$ to MnO, oxidation of MnO to Mn_2O_3, and decomposition of Mn_2O_3 to Mn_3O_4.
5. Siderite, $FeCO_3$, ($\omega = 1.869$, $\epsilon = 1.628$). The specimen is from Lodenstein, Saxony. The curve is characterized by the endothermic decomposition followed by the exothermic oxidation of ferrous oxide to ferric oxide. That the oxidation product was ferric oxide was determined by a powder x-ray picture. The endothermic reaction begins at 500–525°, reaches a peak at 585°, and ends at 605°. The oxidation takes place at 625°, reaches a peak at 735°, and ends at 765°.
6. Siderite, $FeCO_3$, ($\omega = 1.871$, $\epsilon = 1.630$). The specimen is from an unknown locality. The endothermic break is at 515°, reaches a peak at 590°, and ends at 615°. The exothermic break begins at 650°, reaches a peak at 740°, and ends at 790°.
7. Magnesian Siderite (=pistomesite), $(Fe,Mg)CO_3$ (73911), ($\omega = 1.814$, $\epsilon = 1.588$). The specimen is from Traversella, Piedmont, Italy. The decomposition begins very rapidly at 575°, reaches a peak at 580°, and merges with an exothermic curve. The exothermic curve reaches a peak at 725° and ends at 770°. The endothermic break is due to the decomposition of the $FeCO_3$ and $MgCO_3$, and the exothermic curve is due to the oxidation of ferrous oxide to ferric oxide. The area under the exothermic peak corresponds to about 65% $FeCO_3$, a close check with the chemical analysis (Table 7). The decomposition product is the compound magnesio-ferrite, $MgO \cdot Fe_2O_3$, identified by a powder x-ray picture.
8. Smithsonite, $ZnCO_3$, ($\omega = 1.851$, $\epsilon = 1.620$). The specimen is from Magdalena, New Mexico. The decomposition begins slowly at 425°, reaches a peak at 525°, and ends at 550°. The decomposition product is ZnO.

B. *Dolomite series.* The DTA curves for the dolomite series are shown in Fig. 3.

1. Dolomite, $CaMg(CO_3)_2$, ($\omega = 1.684$, $\epsilon = 1.502$). The specimen is from West Roxbury, Vermont. The DTA curve has two endothermic breaks: the first begins at 750°, reaches a peak at 815°, and ends at 845°; the second begins at 855°, reaches a peak at 965°, and ends at 985°. The first peak is due to the decomposition of the $MgCO_3$ part of the dolomite structure and takes place at a temperature 155 degrees higher than the peak temperature for magnesite. The second peak is due to the complete decomposition of the dolomite structure and takes place at a temperature 25 degrees lower than the decomposition peak of calcite. A powder x-ray picture of a sample heated to 850° shows lines of calcite and MgO. The final decomposition product is a mixture of MgO and CaO.
2. Ferroan Dolomite (=ankerite), $Ca(Mg,Fe)(CO_3)_2$ (80383), ($\omega = 1.700$, $\epsilon = 1.519$). The specimen is from Phoenixville, Pennsylvania. The DTA curve is characterized by three endothermic peaks and one exothermic peak. The first endothermic peak is due to the decomposition of the $FeCO_3$ part of the structure; this reaction begins rapidly at 725°, reaches a peak of 740°, an ends at an indeterminate temperature because this curve merges with the exothermic curve due to the oxidation of ferrous oxide to ferric oxide. The exothermic peak is at 785°. The exothermic peak merges slowly with the endothermic peak due to the decomposition of the $MgCO_3$ part of the ankerite structure. This second endothermic peak is at 890°, and this second curve merges with the final endothermic peak due to the complete decomposition of the carbonate. The final curve reaches a peak at 960°. Powder x-ray pictures show the starting ankerite has the same spacing as dolomite, and the final decomposition product is a mixture of CaO and MgO $\cdot Fe_2O_3$ (magnesio-ferrite).
3. Ferroan Dolomite (=ankerite), $Ca(Mg, Fe)(CO_3)_2$, ($\omega = 1.716$, $\epsilon = 1.527$). The specimen is from the Tri-State District. This curve is similar to the ankerite curve discussed above. The differences may be explained by differences in chemical composition. No chemical analysis was made for the Phoenixville ankerite, but the indices of refraction indicate it is lower in $FeCO_3$ than is this Tri-State ankerite specimen. This is reflected in the areas of the iron oxidation break. The final decomposition product is again a mixture of CaO and $MgO \cdot Fe_2O_3$.

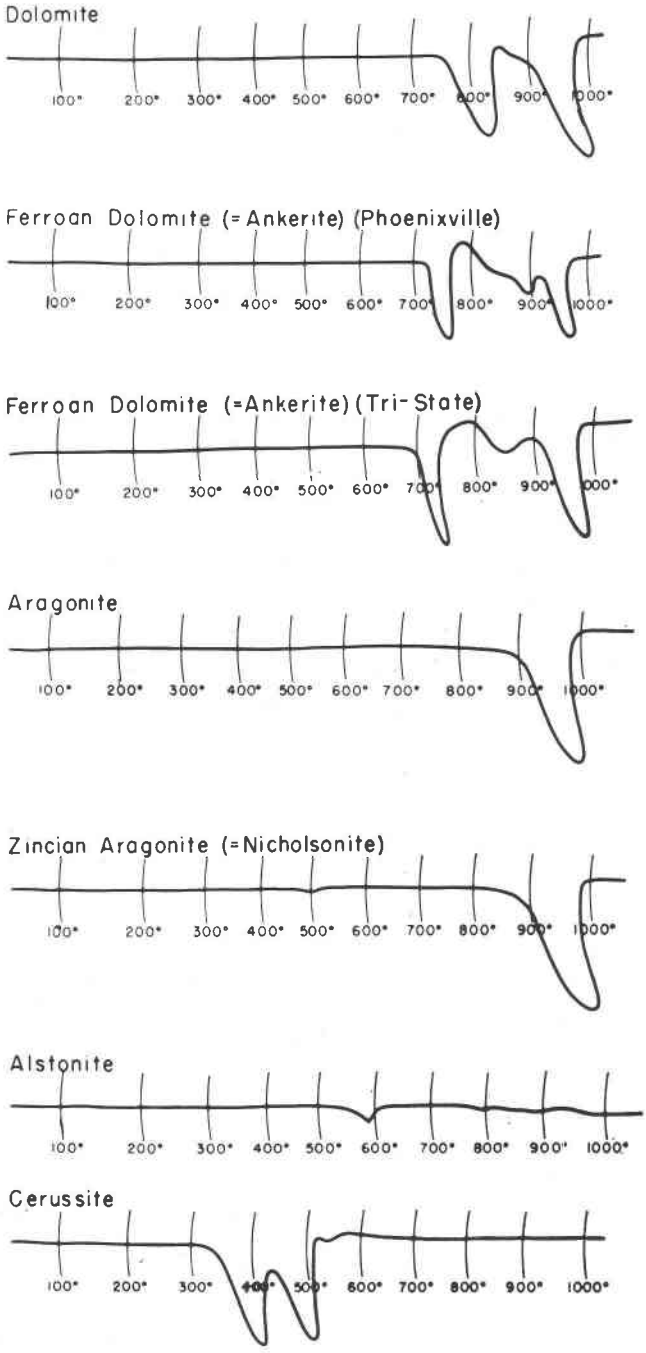

FIG. 3. Differential thermal analysis curves of the dolomite series and the aragonite group.

A powder *x*-ray picture of the product formed when this ankerite is heated to 790° checks no listed compound.

II. *Aragonite Group.* The DTA curves for the aragonite group are shown in Fig. 3.

A. Aragonite, $CaCO_3$, ($\alpha=1.530$, $\beta=1.680$, $\gamma=1.685$). The specimen is from Staditz, Bohemia. The decomposition begins at 850°, reaches a peak at 965°, and returns to the line of zero deflection at 980°. Argonite changes into calcite when heated above 450°. In this study there was no break in the DTA curve to show this transformation. Cuthbert and Rowland (1947) likewise show no inversion point in their aragonite curve. However, recently Faust (1949) reported a small endothermic break in the aragonite curve at 447°.

B. Zincian Aragonite (=nicholsonite), $(Ca,Zn)CO_3$ (90299), ($\alpha=1.532$, $\beta=1.680$, $\gamma=1.688$). The specimen is from Tsumeb, S. W. Africa. The tiny endothermic break at 500° is probably due to the small amount of $ZnCO_3$ in this specimen. A quantitative analysis by the author for $ZnCO_3$ revealed 1.24%. The analysis is not very accurate because of the small amount of sample available, but it reveals the extent of isomorphous substitution of Zn for Ca. The large endothermic break is due to the decomposition of the $CaCO_3$. It begins at 840°, reaches a peak at 970°, and ends at 985°, a close check with pure aragonite.

C. Alstonite (=bromlite), $(Ba,Ca)CO_3$ (80396). The specimen is from Cumberland, England. The DTA curve shows that alstonite is not susceptible to differential thermal treatment with the apparatus used in this investigation because the decomposition of the compound is above the temperature range which can be detected using chromel-alumel differential thermocouples.

The small endothermic break at 585° probably represents a substitution of Mg for Ca and/or Ba. The area corresponds to about 3% $MgCO_3$. Analyses of alstonite reported in Dana's *System of Mineralogy* (Sixth edition, 1892, p. 284) show that Mn is the common substitute for Ca and Ba. However, the break at 585° does not represent the decomposition of $MnCO_3$ because it is not followed by the characteristic exothermic peak (compare rhodochrosite, Fig. 2).

D. Cerussite, $PbCO_3$. The specimen is from Wallace, Idaho. The DTA curve is characterized by a double endothermic break, each part representing approximately the same thermal energy. The decomposition begins at 320°, reaches a peak at 395°, merges

TABLE 3. CHARACTERISTIC THERMAL PEAKS AND AREAS OF THE ANHYDROUS NORMAL CARBONATES

Mineral	Reaction product	Peak temperature, ° C.		Area, mm.²	Weight, gm.	Scale
		Endothermic	Exothermic			
Calcite	CO_2	990		740	0.500	2
Magnesite	CO_2	660		900	0.500	2
Breunnerite	CO_2, MgO	755		860	0.530	2
	Fe_2O_3		785	62		
Rhodochrosite	CO_2	680		595	0.470	2
	Mn_3O_4		795	315		
Siderite (Lodenstein)	CO_2	585		615	0.540	2
	Fe_2O_3		735	320		
Siderite (Loc. unkn.)	CO_2	590		605	0.520	2
	Fe_2O_3		740	295		
Pistomesite	CO_2	580		510	0.580	2
	$MgO \cdot Fe_2O_3$		725	200		
Smithsonite	CO_2	525		495	0.500	2
Dolomite	CO_2	815		315	0.500	2
	CO_2	965		435		
Ankerite (Phoenixville)	CO_2	740		160	0.505	2
	Fe_2O_3		785	45		
	CO_2	890		355		
	CO_2	960				
Ankerite (Tri-State)	CO_2	720		305	0.465	2
	Fe_2O_3		795	20		
	CO_2	850		130		
	CO_2	965		330		
Aragonite	CO_2	965		475	0.410	2
Nicholsonite	CO_2	500		small	0.510	2
	CO_2	970		625		
Cerussite	CO_2	395		810	1.050	2
	CO_2	490				

with the second curve which reaches a peak at 490°, and ends at 510°. The decomposition may take place according to:

$$2PbCO_3 + \text{heat} = PbO \cdot PbCO_3 + CO_2$$
$$PbO \cdot PbCO_3 + \text{heat} = 2PbO + CO_2$$

To test this theory a powder x-ray study was made of decomposition samples taken at 425° and 550°. The sample heated to 550° showed the $PbCO_3$ had decomposed entirely to PbO (litharge). However, the sample heated to 425° gave x-ray lines which were not those of $PbCO_3$, PbO, nor a mixture of $PbCO_3$ and PbO. This gives support to the belief that an oxy-carbonate is formed during the decomposition of cerussite.

Cuthbert and Rowland (1947) report a third endothermic peak at about 860°. They suggest, following Tzentnershver, that the decomposition of cerussite is in three stages: $3PbO \cdot 5PbCO_3$, $2PbO \cdot PbCO_3$, and $PbO \cdot PbCO_3$. The author did not get the third peak; furthermore, the x-ray picture at 550° shows complete decomposition to PbO.

Hydrous Normal Carbonates

The DTA curves of the hydrous normal carbonates are shown in Fig. 4.

Gay-Lussite, $CaCO_3 \cdot Na_2CO_3 \cdot 5H_2O$ (76971), ($\alpha = 1.445$, $\beta = 1.515$, $\gamma = 1.522$). The specimen is from Lagunillo, Maracaibo, Venezuela. The DTA curve shows an overlapping endothermic doublet at 145° and 175° due to the loss of the water of crystallization in two distinct stages. The remainder of the curve is highly irregular due to the slow fusing of the mineral.

Nesquehonite, $MgCO_3 \cdot 3H_2O$ (77292), ($\alpha = 1.412$, $\beta = 1.501$, $\gamma = 1.526$). The specimen is from No. 2 Tunnel, Nesquehoning Carbon Company, Nesquehoning, Pennsylvania. The doublet endothermic curve is due to the loss of two molecules of water of crystallization. This reaction begins at 140°, reaches a double peak at 210–235°, and ends at 300°. The second endothermic curve is due to the loss of a third molecule of water. This reaction begins at 380°, reaches a peak at 425°, and ends at 475°. Powder x-ray studies indicate that this second reaction results in a seemingly amorphous MgO decomposition product. The decomposition of the remaining carbonate begins at 480°, reaches a doublet peak at 535° and 585°, and ends at 620°. The inversion of the amorphous (?) MgO to cubic MgO is superimposed upon the last endothermic reaction and is shown by the exothermic peak at 510°. By analogy with hydromagnesite and artinite (Fig. 6), the loss of the third molecule of water is like the loss of

basic water. The formula, therefore, might better be written $Mg(HCO_3)(OH)\cdot 2H_2O$, which would make the intermediate decomposition $Mg(HCO_3)(OH)$. Davis (1906) confirms this on artificial $MgCO_3\cdot 3H_2O$. He reports that the third molecule of water comes off with the evolution of CO_2.

Optical and powder x-ray studies were made on the decomposition

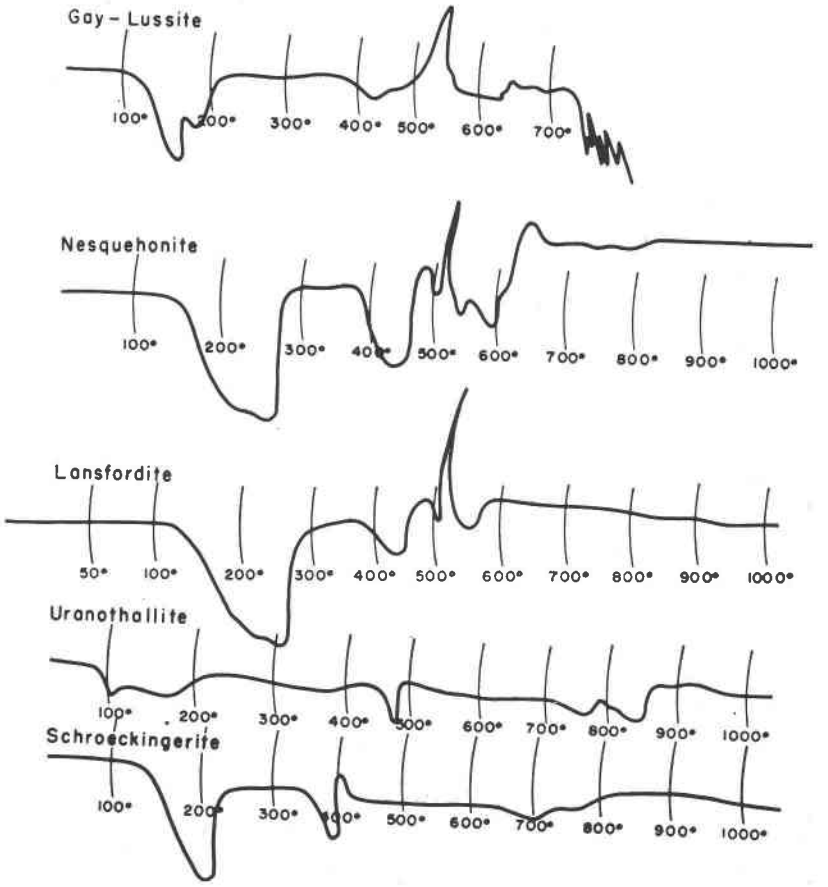

FIG. 4 Differential thermal analysis curves of the hydrous normal carbonates.

products when nesquehonite was heated to 325°, 470°, 515°, and 1000°. The 325° product gives the spacing of no listed compound. Most of the grains retain an orthorhombic external shape. They are diffused, but no amorphous material is present. A few of the grains are still nesquehonite, some are mostly decomposed but retain a little nesquehonite, but most are entirely decomposed. Average $n=1.425$. The 470° product gives the

spacing of no listed compound. There is a broad, amorphous band at $d = 2.45$ Å. Optically the product appears isotropic with $n =$ about 1.545. The 515° product shows periclase lines. The 1000° product is periclase.

TABLE 4. CHARACTERISTIC THERMAL PEAKS AND AREAS OF THE HYDROUS NORMAL CARBONATES

Mineral	Reaction product	Peak temperature, °C.		Area, mm.²	Weight, gm.	Scale
		Endothermic	Exothermic			
Gay-Lussite	H_2O	145		400	0.250	3
	H_2O	175				
Nesquehonite	H_2O	210–235		865	0.280	3
	OH^-	425		355		
	MgO?		510	small		
	CO_2	535–585		355		
Lansfordite	H_2O	210–235		760	unknown	3
	OH^-	440		155		
	MgO?		510	small		
	CO_2	555		100		
Uranothallite	?	110		170	0.140	3
	?	175				
	?	475		65		
	?	750		140		
	?	890				
Schroeckingerite	?	190		400	0.295	3
	?	385		75		
	?		410	15		
	?	700		indefinite		

Lansfordite, $MgCO_3 \cdot 5H_2O$ (77072). The specimen is from the No. 2 Tunnel, Nesquehoning Carbon Company, Nesquehoning, Pennsylvania. The sample required special treatment to make the run. Lansfordite rapidly loses two molecules of water on standing at room temperature to form nesquehonite. The mineral specimen at Harvard had been kept under oil. To ready it for a differential thermal analysis run the specimen was cleaned with ether and kept under ether. The run was started from room temperature instead of 50°. Because only enough sample was available to fill about $\frac{1}{5}$ of the sample hole, the hole was partly filled with inert alumina, then the lansfordite was packed around the thermojunction, and the remainder of the hole was filled with more alumina.

The reaction begins at 115°, reaches a doublet peak at 210–230°, and ends at 275°. This curve is due to the volatilization of four molecules of water. The second endothermic curve, due to the loss of a fifth molecule of water, begins at 375°, reaches a peak at 440°, and ends at 480°. The exothermic peak at 510°, by analogy with nesquehonite, is the inversion of amorphous (?) MgO to cubic MgO. The third endothermic curve is due to the loss of CO_2. It begins at 490°, reaches a peak at 555°, and ends at 575°. Unlike nesquehonite, this latter deflection has but one peak.

Uranothallite, $Ca_2U(CO_3)_4 \cdot 10H_2O$ (?) (94861). The specimen is from Joachimsthal, Bohemia. Any interpretation of the DTA curve would be speculative because (1) not enough material was available to permit the stopping of a run at different phases, and (2) the composition of this, and other uranium carbonates is not definitely determined.

Schroeckingerite, $NaCa_3(UO_2)(CO_3)_3(SO_4)F \cdot 10H_2O$. The specimen is from near Wamsutter, Wyoming, and is Larsen's (Larsen and Gonyer, 1937) type material. Again the interpretation of the DTA curve is difficult and is presented without comment. The above formula was assigned to schroeckingerite by Jaffe, Sherwood, and Peterson (1948), and verified in the laboratory of the U. S. Geological Survey by F. S. Grimaldi (in press). A powder x-ray picture of the final decomposition product is the same as the end product of the decomposition of uranothallite.

Carbonates Containing Hydroxyl or Halogen

Bastnäsite Group. The DTA curves of the bastnäsite group are shown in Fig. 5.

I. Bastnäsite, $CeFCO_3$ (88742), ($\omega = 1.719$, $\epsilon = 1.820$). The specimen is from Ampanbabe, Madagascar. The DTA curve shows that the loss of CO_2 begins slowly at 350°, has a characteristic shoulder at 470°, and reaches a peak at 625°. The endothermic curve merges with an exothermic curve. The latter reaches a peak at 650° and is due to the oxidation of cerous oxide to ceric oxide. Fluorine is lost during the run as shown by a slight attack on the nickel cover.

An x-ray picture of the final decomposition product gives the structure of CeO_2, but other lines suggest the presence of isostructural RO_2, where R = other rare earth elements.

II. Bastnäsite, $CeFCO_3$ (84440), ($\omega = 1.719$, $\epsilon = 1.820$). The specimen is from St. Peter's Dome, El Paso County, Colorado. The DTA curve is practically identical with that of the Madagascar bastnäsite.

III. "Tysonite," $(Ce,La,Di)F_3$ (82848), ($\omega = 1.718$, $\epsilon = 1.818$). The specimen, labeled "tysonite," is from Colorado. The DTA curve shows that the specimen is bastnäsite. The curve is practically identical with those of the two foregoing bastnäsite samples. Most bastnäsite is pseudomorphic after tysonite; therefore, the error in identification is not unnatural.

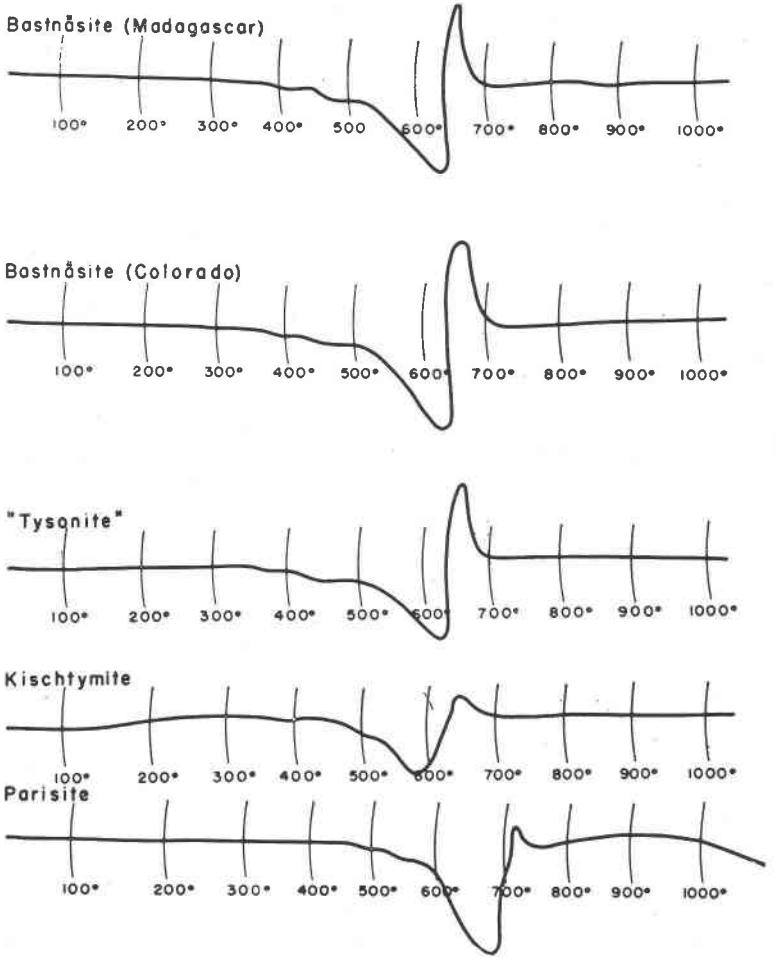

FIG. 5. Differential thermal analysis curves of the bastnäsite group.

IV. Kischtymite (= hydroxyl bastnäsite?) (84435), ($\omega = 1.711$, $\epsilon = 1.812$). The specimen is from Kischtymsk, U.S.S.R. The kischtymite DTA curve is similar to the bastnäsite curves. The smaller areas under the curves probably are due to the smaller amount of the mineral

that was available for analysis. Decomposition begins slowly about 360°, and reaches a peak at 580°. This peak is 40–45° lower than the corresponding bastnäsite peak; this may be partly, or entirely due to the smaller charge, or it may reflect a characteristic difference between kischtymite and bastnäsite. The end of the reaction is slower than in the case of the bastnäsites, and as a result the peak of the exothermic curve due to the oxidation of cerous to ceric oxide comes at the characteristic temperature, namely, 650°. From DTA alone kischtymite would be classified as bastnäsite.

V. Parisite, $2CeFCO_3 \cdot CaCO_3$ (11019), ($\omega = 1.675$, $\epsilon = 1.755$). The specimen is from Muso, Colombia. The decomposition begins at 470°, and reaches a peak at 660°. This endothermic curve merges with an exothermic curve that reaches a peak at 720°. The exothermic peak again represents the oxidation of cerous to ceric oxide. At 975° an endothermic break begins slowly; the run was stopped at 1100° and before the peak was reached.

The DTA curves for the remainder of the carbonates containing hydroxyl or halogen are shown in Figs. 6, 7, and 8.

Hydromagnesite, $3MgCO_3 \cdot Mg(OH)_2 \cdot 3H_2O$ (84570), ($\alpha = 1.522$, $\beta = 1.528$, $\gamma = 1.545$). The specimen is from Alameda, California. The decomposition begins slowly at 275–325° with the loss of the water of crystallization, reaches a peak at 375°, and merges with the curve representing the loss of basic water. The latter curve reaches a peak at 440°. These reactions result in the formation of amorphous (?) MgO which inverts to cubic MgO at 510° as shown by the exothermic curve. The loss of CO_2 begins at 485°, reaches a doublet peak at 565° and 600°, and ends at 610°. This curve is similar to the curves discussed above for nesquehonite and lansfordite save in this case the water of crystallization comes off at a higher temperature, high enough to overlap the loss of hydroxyl water.

Artinite, $MgCO_3 \cdot Mg(OH)_2 \cdot 2H_2O$, ($\alpha = 1.489$, $\beta = 1.534$, $\gamma = 1.556$). The specimen is from Luning, Nevada. The decomposition begins at 230° with the loss of the water of crystallization, reaches a peak at 280°, and ends at 305°. The loss of hydroxyl water begins at 385°, reaches a peak at 440°, and merges with the curve due to the loss of CO_2. This latter reaction has a peak at 540°, a characteristic shoulder at 575°, and ends at 585°. Superimposed upon this latter curve is an exothermic reaction which is of smaller magnitude than those recognized in nesquehonite, lansfordite, and hydromagnesite. However, this exothermic curve reaches a peak at 510°, and it is believed that it represents an inversion of amorphous (?) MgO to cubic MgO. The loss of the water of crystal-

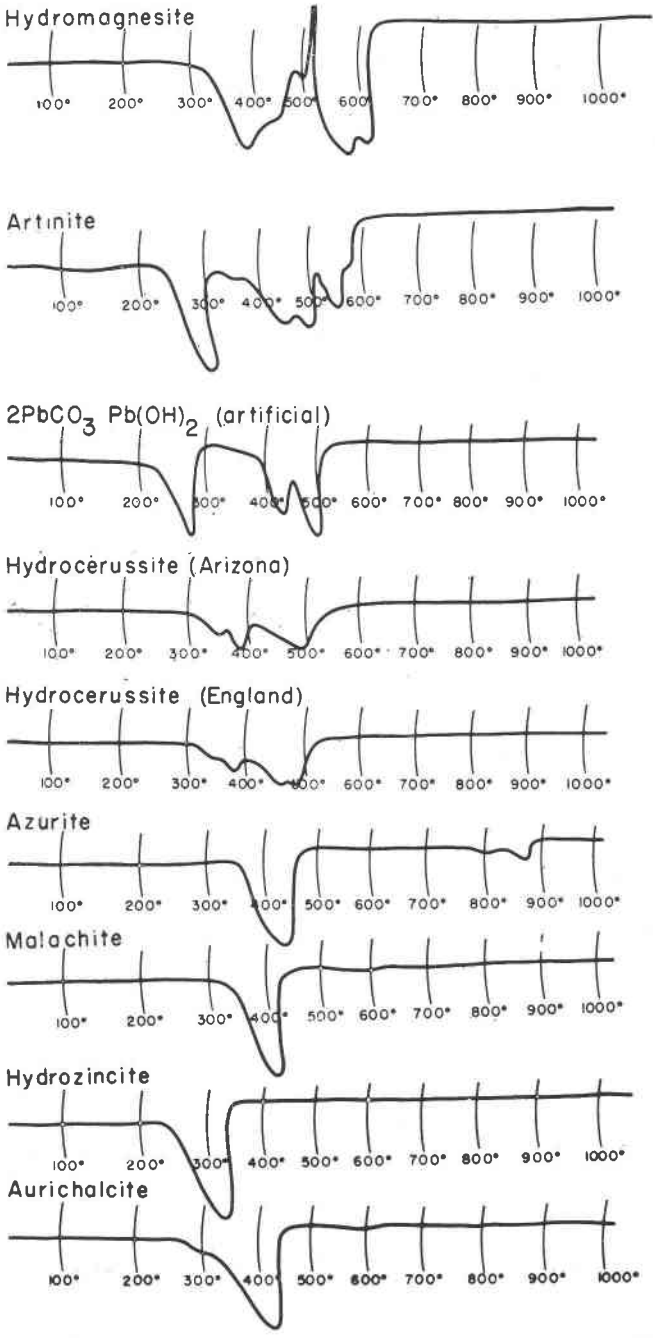

FIG. 6. Differential thermal analysis curves of carbonates containing hydroxyl.

lization is at a lower temperature than the corresponding reaction in hydromagnesite.

Hydrocerussite (artificial), $2PbCO_3 \cdot Pb(OH)_2$. The loss of hydroxyl water begins at 235°, reaches a peak at 270°, and ends at 290°. The decomposition of the carbonate is shown by the double endothermic break beginning at 380°, reaching peaks at 430° and 490°, and ending at 505°. This doublet peak is analogous to the decomposition of cerussite, and is likewise probably due to the formation of an intermediate oxy-carbonate before complete decomposition.

Hydrocerussite, $2PbCO_3 \cdot Pb(OH)_2$. The specimen is from Mammoth Mine, Arizona. The loss of hydroxyl water begins at 280–300°, reaches a peak at 345°, and merges with the double peak due to the loss of CO_2. This doublet reaches peaks at 385° and 500°, and ends at 550°. The natural hydrocerussite, therefore, loses its water at a temperature 75° higher than the artificial compound. On the other hand the first peak of the loss of CO_2 in the natural compound is at a temperature 45° lower than in the artificial compound, while the peak of the final decomposition is at approximately the same temperature for both.

Hydrocerussite, $2PbCO_3 \cdot Pb(OH)_2$. The specimen is from Mendip Hills, Somerset, England. The loss of hydroxyl water begins at 295° and merges completely with the first curve of the decomposition of the carbonate part of the structure. This latter reaction reaches a peak at 380° and merges with the second characteristic peak of the decomposition of $PbCO_3$. This second curve reaches a peak at 485°. The DTA curve for this specimen of hydrocerussite agrees very well with the run for the Arizona hydrocerussite.

Azurite, $2CuCO_3 \cdot Cu(OH)_2$, ($\alpha = 1.730$, $\beta = 1.758$, $\gamma = 1.838$). The specimen is from Tsumeb, S. W. Africa. The loss of hydroxyl water and CO_2 takes place in one endothermic break. The decomposition begins at 350°, reaches a peak at 430°, and ends at 475°. The decomposition product is tenorite, CuO, identified by a powder x-ray picture. The endothermic doublet at 850° and 930° is due to an admixture of dolomite.

Malachite, $CuCO_3 \cdot Cu(OH)_2$, ($\alpha = 1.655$). The specimen is from Tsumeb, S. W. Africa. The loss of water and CO_2 takes place in one endothermic break. The decomposition begins at 315°, reaches a peak at 385°, and ends at 420°. This decomposition takes place at a temperature 45 degrees lower than does the decomposition of azurite. The loss of hydroxyl water occurs at a lower temperature than does the loss of CO_2 in most compounds; and, since there is more hydroxyl water in malachite than in azurite, it is to be expected that the former would decompose at a lower

temperature than the latter. The decomposition product is again tenorite.

Hydrozincite, $2ZnCO_3 \cdot 3Zn(OH)_2$ (85740), ($\alpha = 1.636$, $\beta = 1.728$, $\gamma = 1.740$). The specimen is from Cumillas, Spain. The loss of hydroxyl water and CO_2 takes place in one endothermic break. The decomposition begins at 230°, reaches a peak at 310°, and ends at 340°. The decomposition product is zincite, ZnO.

Aurichalcite, $2(Zn,Cu)CO_3 \cdot 3(Zn,Cu)(OH)_2$ (80960). The specimen is from the Big Cottonwood District, Utah. The loss of hydroxyl water and CO_2 takes place in one endothermic break. The decomposition begins at 275°, has a characteristic shoulder at 300°, reaches a peak at 415°, and ends at 445°. The final decomposition product is a mixture of tenorite and zincite, with zincite dominating.

Bismutite, Bi_2CO_5 (84598). The specimen is from Engle Station,* New Mexico. The decomposition curve consists of a large endothermic break and a small endothermic break. The decomposition begins at 420°, reaches a peak at 495°, and ends at 520°. The smaller break begins immediately, reaches a peak at 605°, and ends at 640°. The third endothermic peak is due to the inversion of Bi_2O_3; it begins at 640° and reaches a peak at 710°. A powder x-ray picture shows the final decomposition product to be γ-Bi_2O_3, the body-centered cubic polymorph (Schumb and Rittner, 1943).

Bismutite, Bi_2CO_5 (90756). The specimen is from Petaca, New Mexico. The decomposition curve consists of two merging endothermic breaks. The decomposition begins at 400°, reaches a peak at 530°, merges with the second curve which reaches a peak at 625°, and ends at 695°. These temperatures are 20–50 degrees higher than the corresponding reactions in the Engle Station bismutite. The small endothermic peak at 730° is due to the inversion of the decomposition product, Bi_2O_3. That this is an inversion is shown by a cooling curve which gives the reinversion at about 715°.

Powder x-ray pictures of samples heated to 560° and 640° are identical with β-Bi_2O_3, the tetragonal or pseudocubic high temperature polymorph (Schumb and Rittner, 1943). Therefore, the second endothermic break is believed to be an inversion of β-Bi_2O_3 to an undetermined polymorph which changes back to β-Bi_2O_3 on cooling to room temperature.

Powder x-ray pictures of samples heated to 700° and 750° are identical and consist of a mixture of β-Bi_2O_3 and the simple cubic polymorph. The

* Presumably from the Grandview Canyon district, San Andres Mountains, New Mexico.

lines check very well with the spacing reported by Sillén (1938). Sillén reports that β-Bi_2O_3 kept molten several hours changes to a simple cubic polymorph. This transformation takes place only if impurities, such as silica, are present.

Bismutite, Bi_2CO_5. The specimen is from Willimantic, Connecticut. The DTA curve is similar to the DTA curve for the Engle Station, New Mexico bismutite. The decomposition begins at 400°, reaches a peak at 480°, and ends at 530°. The second endothermic curve begins at 135°, reaches a peak at 600°, and ends at 650°.

Powder *x*-ray pictures of samples heated to 525° and 700° are identical with γ-Bi_2O_3, the body-centered cubic polymorph. Again, the second endothermic break seems to represent an inversion which reinverts on cooling.

DTA curves were run on artificial Bi_2O_3 and bismite (Fig. 7). Powder *x*-ray pictures of both, before and after heating, give the spacing of α-Bi_2O_3, the monoclinic polymorph (Sillén, 1938; Schumb and Rittner, 1943). The inversion and reinversion of artificial Bi_2O_3 are shown on the DTA curve.

In summary, the first endothermic break in the DTA runs of the bismutite minerals is due to the loss of CO_2. The smaller second endothermic break probably represents an undetermined inversion. Sillén (1938) reports that such inversions are facilitated by the presence of silica impurities. A DTA run on C.P. artificial Bi_2CO_5 did not show the second endothermic break; presumably it is free of any impurities. All the bismutites show another inversion around 725° to form β-Bi_2O_3, a mixture of β-Bi_2O_3 and the simple cubic polymorph, or γ-Bi_2O_3.

Beyerite, $(Ca,Pb)Bi_2(CO_3)_2O_2$. The specimen is from Fremont County, Colorado, and was supplied by E. Wm. Heinrich (Heinrich, 1947). The DTA curve shows a large endothermic break which begins at 485°, reaches a peak at 570°, and ends at 625°. A second endothermic curve begins at 660°, reaches a peak at 675°, and ends at 700°. The DTA curve shows the start of another endothermic break at 725°; this is the start of the inversion of Bi_2O_3. A powder *x*-ray picture of the final product shows that it is β-Bi_2O_3.

The beyerite curve is similar to the bismutite curves, but the peaks are 50–75 degrees higher for the beyerite breaks. The energy associated with the first endothermic break is greater for beyerite than for bismutite. Again, it is believed that the first endothermic break is due to the loss of CO_2, and the second endothermic break is an undetermined inversion.

Rutherfordine, UO_2CO_3 (?) (89472). The specimen is from Morogoro, Tanganyika Territory, Africa. The formula of rutherfordine is open to question, and any interpretation of the DTA curve would be speculative.

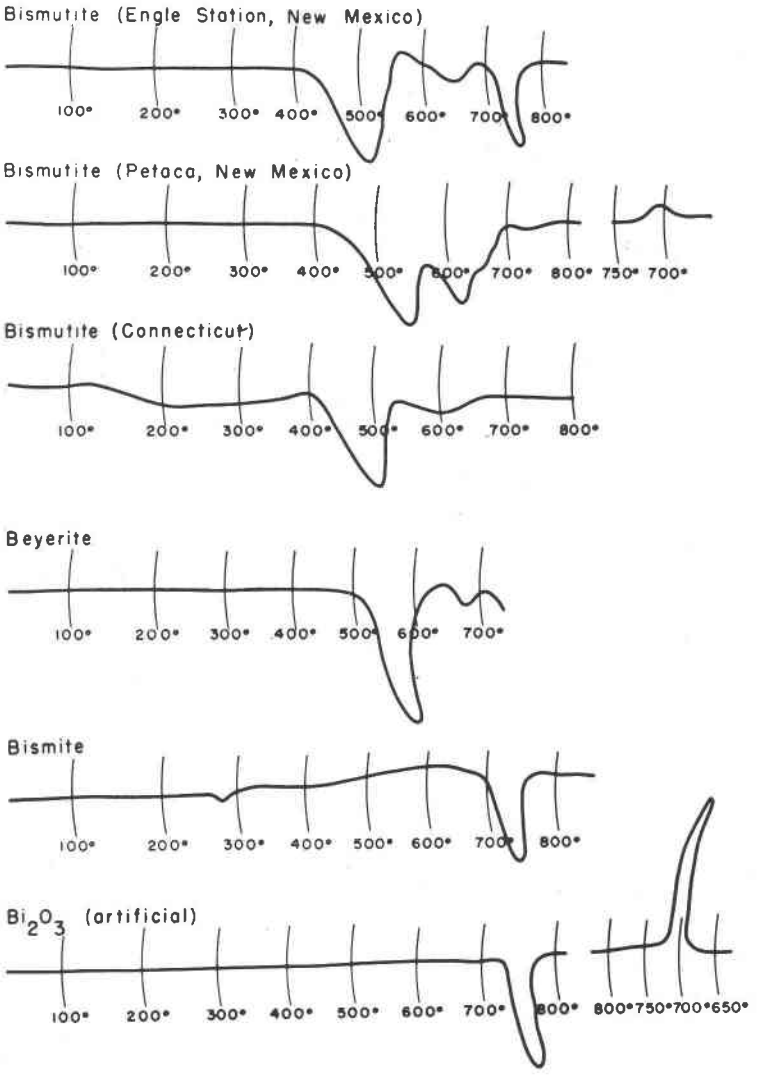

FIG. 7. Differential thermal analysis curves of some bismuth minerals.

Powder *x*-ray pictures of the final decomposition product show the same lines as the decomposition products of uranothallite and schroeckingerite, but with slightly different spacings.

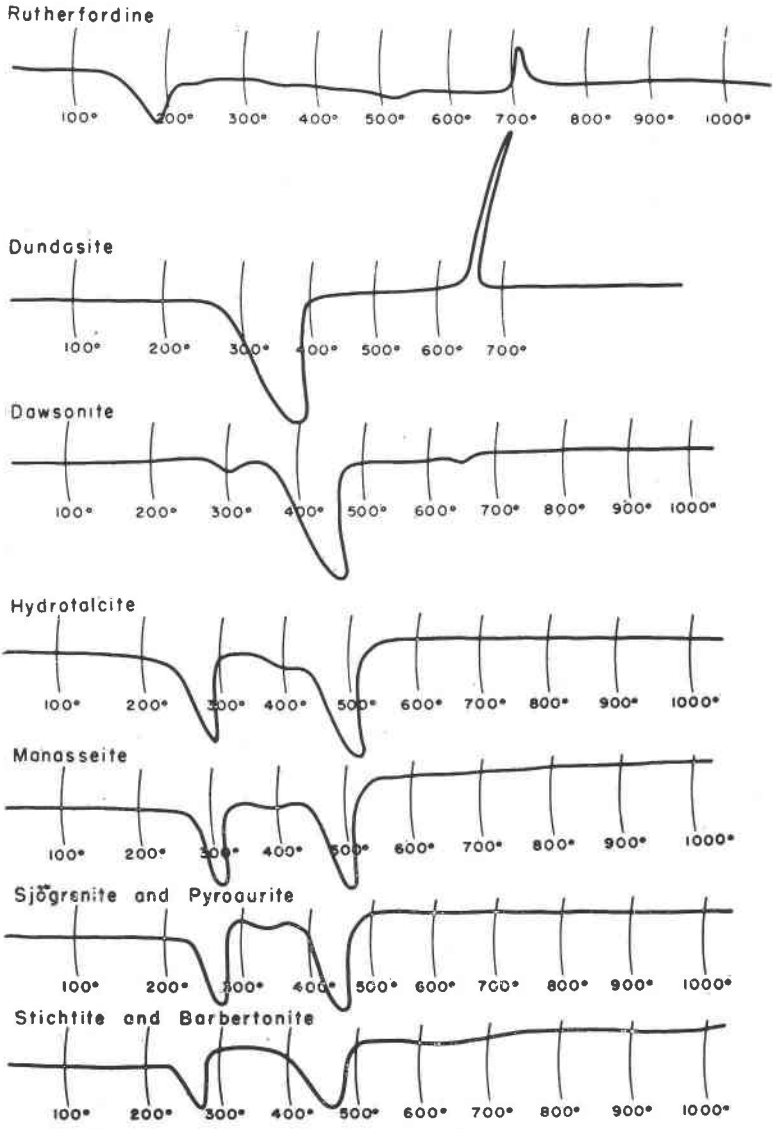

FIG. 8. Differential thermal analysis curves of rutherfordine, dundasite, dawsonite, the pyroaurite group, and the sjögrenite group.

Dundasite, $Pb(AlO)_2(CO_3)_2 \cdot 4H_2O$ (84578). The specimen is from Dundas, Tasmania. The loss of water of crystallization and CO_2 takes place in one endothermic reaction. This reaction begins at 250°, reaches a peak at 350°, and ends at 400°. A powder x-ray picture of the decomposition

product at 500° shows it to be amorphous. A probable inversion is shown by the exothermic peak at 660°. The run was stopped at 700° to avoid fusing the PbO. A powder x-ray picture of the mineral heated to 700° gives lines corresponding to neither Al_2O_3 nor PbO.

Dawsonite, $Na_3Al(CO_3)_3 \cdot 2Al(OH)_3$ (91177), ($\alpha = 1.465$, $\beta = 1.540$, $\gamma = 1.598$). The specimen is from Montreal, Canada. The small endothermic break which begins at 275°, reaches a peak at 300°, and ends at 315° is due to the loss of non-essential water from the structure. The optics and powder x-ray picture of a sample heated to 325° are identical with the starting mineral. The large endothermic break is the loss of hydroxyl water and CO_2. This reaction begins at 345°, reaches a peak at 440°, and ends at 470°.

Hydrotalcite, $MgCO_3 \cdot 5Mg(OH)_2 \cdot 2Al(OH)_3 \cdot 4H_2O$, ($\omega = 1.512$, $\epsilon = 1.498$). The specimen is from Snarum, Norway. The first endothermic reaction might be the loss of the four molecules of water of crystallization. This reaction begins slowly from 200–240°, reaches a peak at 285°, and ends at 300°. A small endothermic reaction begins at 350°, reaches a peak at 405°, and overlaps a large endothermic reaction which reaches a peak at 495°, and ends at 520°. The 405° peak is believed to be the loss of basic water from $Al(OH)_3$, and the 495° peak is believed to be the loss of basic water and CO_2 from $Mg(OH)_2$ and $MgCO_3$.

A powder x-ray picture of the 1000° decomposition product gives the spacing of periclase with no evidence of alumina.

Manasseite, $MgCO_3 \cdot 5Mg(OH)_2 \cdot 2Al(OH)_3 \cdot 4H_2O$ (87211), ($\omega = 1.524$, $\epsilon = 1.510$). The specimen is from Snarum, Norway. The first endothermic reaction might be the loss of four molecules of water of crystallization. This reaction begins at 275°, reaches a peak at 315°, and ends at 340°. A small endothermic reaction begins at 360°, reaches a peak at 400°, and overlaps a large endothermic reaction which reaches a peak at 495°, and ends at 535°.

Manasseite and hydrotalcite are polymorphs and their differential thermal curves are similar. The main difference is in the temperature at which the water of crystallization is lost; the manasseite peak is 30° higher than the hydrotalcite peak. The other two endothermic peaks are practically identical for the two minerals.

Pyroaurite and Sjögrenite, $MgCO_3 \cdot 5Mg(OH)_2 \cdot 2Fe(OH)_3 \cdot 4H_2O$ (83907), ($\omega = 1.572$, $\epsilon = 1.549$). These two polymorphous minerals occur in a specimen from Långban, Sweden. They are isostructural with hydrotalcite and manasseite respectively (Frondel, 1941). The estimated ratio of pyroaurite:sjögrenite in the specimen is 1:9.

The DTA curve is a combination of the curves of pyroaurite and sjögrenite. The same three endothermic curves which were characteristic of hydrotalcite and manasseite are also characteristic of the pyroaurite-sjögrenite mixture, but they reach peaks at different temperatures. The loss of the four molecules of water of crystallization begins at 215°, reaches a peak at 270°, and ends at 290°. The small endothermic break begins at 295°, reaches a peak at 350°, and overlaps the large endothermic break which reaches a peak at 455°, and ends at 500°. This DTA curve is dominated by sjögrenite. By analogy with hydrotalcite and manasseite, a curve of pyroaurite would lose the water of crystallization at a temperature slightly lower than the curve of the pyroaurite-sjögrenite mixture.

Stichtite and Barbertonite, $MgCO_3 \cdot 5Mg(OH)_2 \cdot 2Cr(OH)_3 \cdot 4H_2O$ (92549), ($\omega = 1.551$, $\epsilon = 1.523$). These two polymorphous minerals are from the Transvaal, South Africa. Stichtite is isostructural with hydrotalcite and pyroaurite; barbertonite, with manasseite and sjögrenite (Frondel, 1941). The estimated ratio of stichtite:barbertonite is 1:1. Unlike the DTA curves of the other minerals of this group, this DTA curve shows only two endothermic breaks—the small one is absent. The loss of the four molecules of water of crystallization begins at 235°, reaches a peak at 275°, and ends at 290°. The second endothermic curve begins slowly at 360°, reaches a peak at 455°, and ends at 500°. These two peaks, therefore, correspond closely with the hydrotalcite, manasseite, and pyroaurite-sjögrenite curves. By analogy with hydrotalcite it would be expected that stichtite would lose its water of crystallization at a peak slightly below 275°.

This DTA curve enables one to interpret the three preceding curves, especially the small endothermic break. The first break in all cases is believed to be the loss of four molecules of water of crystallization. The small endothermic reaction represents the loss of hydroxyl water from the trivalent cation; in the case of stichtite-barbertonite this break is either higher or lower and overlaps the last or first endothermic break; that is, the loss of hydroxyl water from $Cr(OH)_3$ is at a higher or lower temperature than the corresponding loss in $Al(OH)_3$ and $Fe(OH)_3$. The last endothermic reaction is the loss of hydroxyl water from the $Mg(OH)_2$ plus the loss of CO_2 from $MgCO_3$.

Frondel (1941) discusses the constitution and polymorphism of the pyroaurite and sjögrenite groups. Pyroaurite, stichtite, and hydrotalcite belong to the rhombohedral or pyroaurite group. The cell dimensions and the indices of refraction decrease from pyroaurite to hydrotalcite. Sjögrenite, barbertonite, and manasseite belong to the hexagonal or sjögrenite group. The cell dimensions and indices of refraction decrease

TABLE 5. CHARACTERISTIC THERMAL PEAKS AND AREAS OF THE CARBONATES CONTAINING HYDROXYL OR HALOGEN

Mineral	Reaction product	Peak temperature, °C.		Area, mm.²	Weight, gm.	Scale
		Endothermic	Exothermic			
Bastnäsite, Ampanbabe	CO_2, F_2 CeO_2	625	650	500 110	0.800	2
Bastnäsite Colorado	CO_2, F_2 CeO_2	620	655	530 190	0.810	2
"Tysonite" (Bastnäsite)	CO_2, F_2 CeO_2	625	650	460 140	0.795	2
Kischtymite	CO_2, F_2 CeO_2	580	650	275 30	0.630	2
Parisite	CO_2, F_2 CeO_2	660	720	530 20	0.770	2
Hydromagnesite	H_2O OH^- MgO CO_2 CO_2	375 440 565 600	510	 595 small 710	0.325	3
Artinite	H_2O OH^- CO_2 MgO CO_2	280 440 480 540	510	340 675 small	0.265	3
$2PbCO_3 \cdot Pb(OH)_2$ (artificial)	H_2O CO_2 CO_2	270 430 490		215 395	0.680	2
Hydrocerussite (Arizona)	H_2O CO_2 CO_2	345 385 500		420	0.960	2
Hydrocerussite (England)	H_2O CO_2 CO_2	345 380 485		350	0.575	2
Azurite	H_2O, CO_2	430		440	0.550	2
Malachite	H_2O, CO_2	385		380	0.580	2

TABLE 5. *Continued*

Mineral	Reaction product	Peak temperature, °C.		Area, mm.²	Weight, gm.	Scale
		Endothermic	Exothermic			
Hydrozincite	H_2O, CO_2	310		535	0.355	2
Aurichalcite	H_2O, CO_2	415		540	0.315	2
Bismutite (Engle Station)	CO_2 Inversion? γ-Bi_2O_3	495 605 710		440 80 ?	0.875	3
Bismutite (Pectaca)	CO_2 Inversion? Simple cubic and β-Bi_2O_3	530 625 730		820	0.960	3
Bismutite (Willimantic)	CO_2 Inversion?	480 600		340 60	1.000	3
Beyerite	CO_2 Inversion? β-Bi_2O_3	570 675 725		380 35 ?	0.490	3
Rutherfordine	? ?	190	715	130 20	0.225	3
Dundasite	H_2O, CO_2 ?	350	660	620 75	0.340	2
Dawsonite	H_2O OH^-, CO_2	300 440		20 415	0.390	2
Hydrotalcite	H_2O OH^- OH^-, CO_2	285 405 495		235 385	0.285	2
Manasseite	H_2O OH^- OH^-, CO_2	315 400 495		180 330	0.325	2
Pyroaurite & Sjögrenite	H_2O OH^- OH^-, CO_2	270 350 455		195 325	0.295	2
Stichtite & Barbertonite	H_2O OH^-, CO_2	275 455		110 215	0.210	2

TABLE 6. CHARACTERISTIC THERMAL PEAKS AND AREAS OF THE COMPOUND CARBONATES, WITH SULFATES, HALIDES

Mineral	Reaction product	Peak temperature, °C. endothermic	Area, mm.²	Weight, gm.	Scale
Phosgenite	CO_2	435	175	0.930	2
Leadhillite	H_2O, CO_2	345	150	0.850	2
	CO_2	485	65		

TABLE 7. CHEMICAL ANALYSES OF SOME OF THE CARBONATE MINERALS

Mineral	Locality	% metallic oxide	% CO_2	% H_2O	Analyst
Calcite	Canada	CaO —56.17	43.72		Carl W. Beck
Magnesite	Austria	MgO—46.91 CaO—0.58	52.13		Carl W. Beck
Breunnerite	California	MgO—39.62 FeO — 9.51 CaO — 0.43	49.74		Carl W. Beck
Rhodochrosite	Montana	MnO—56.98 FeO — 0.34	38.78		F. A. Gonyer
Siderite	Saxony	FeO —52.6 MnO—10.4	38.5		H. R. Shell
Pistomesite	Italy	FeO —42.58 MgO—14.18 MnO— 0.39	41.75		F. A. Gonyer
Ankerite	Tri-State	CaO —30.68 FeO —11.64 MgO—10.80 MnO— 1.71	44.28		F. A. Gonyer
Artinite	Nevada	MgO—41.81	22.82	35.46	F. A. Gonyer
Beyerite	Colorado	Bi_2O_3—73.65 CaO — 8.85 PbO — 1.73 CuO — 1.10 MnO— 0.12	13.59	0.79 (insol.)	F. A. Gonyer

from sjögrenite to mansaseite. A similar, but less well-defined, parallel change takes place in the peak temperatures of the DTA curves of the members of the pyroaurite and sjögrenite groups. The members that have the smallest cell dimensions have the highest peak temperatures; that is, the decomposition reactions of hydrotalcite take place at a temperature higher than corresponding reactions in stichtite, and the reactions of stichtite are, in turn, higher than those of pyroaurite. Similarly, the decomposition reactions of manasseite take place at a temperature higher than the corresponding reactions in barbertonite, and the reactions of barbertonite are, in turn, higher than those of sjögrenite.

Compound Carbonates, with Sulfates, Halides

The DTA curves for the compound carbonates, with sulfates, halides are shown in Fig. 9.

Phosgenite, $PbCO_3 \cdot PbCl_2$ (84449). The specimen is from Monte Poni, Sardinia. The decomposition due to the loss of CO_2 becomes rapid at 360°, though the reaction may have begun slowly a hundred degrees earlier. The reaction reaches a peak at 435°, and ends at 445°. The second endothermic break is due to the melting of the decomposition product. Powder x-ray pictures of samples heated to 475° and 590° are identical. The pattern corresponds to neither PbO, $PbCl_2$, nor a mixture of the two.

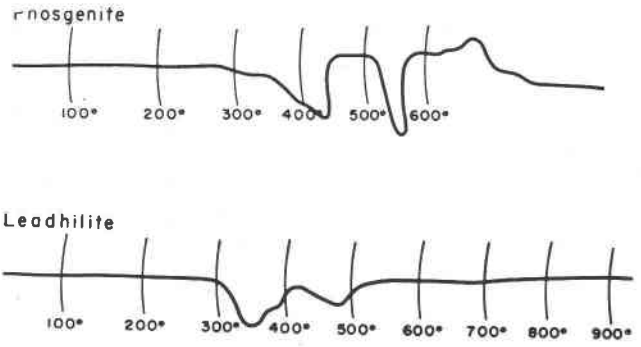

FIG. 9. Differential thermal analysis curves of phosgenite and leadhillite.

Leadhillite, $2PbCO_3 \cdot 2Pb(OH)_2 \cdot PbSO_4$. The specimen is from Eureka Mine, Utah. The decomposition of leadhillite is similar to the decomposition of hydrocerussite (Fig. 3). The loss of hydroxyl water begins at 300°, reaches a peak at 345°, and merges almost completely with the first stage in the decomposition of the $PbCO_3$ part of the structure, and ends at 400°. There is a characteristic shoulder at 375°. The total decomposition of the carbonate begins at 420°, reaches a peak at 485°, and ends at 520°. A powder x-ray picture of a sample heated to 600°

gives a pattern corresponding to neither PbO, $PbSO_4$, nor a mixture of the two.

ACKNOWLEDGMENT

The author wishes to acknowledge the interest and encouragement shown by Professors E. S. Larsen, Jr., C. S. Hurlburt, Jr., and Clifford Frondel of the Department of Mineralogy and Petrography, Harvard University. He is especially indebted to Dr. Michael Fleischer, U. S. Geological Survey, for helpful suggestions and critical reading of the manuscript.

REFERENCES

BECK, CARL W. (1950), An amplifier for differential thermal analysis: *Am. Mineral.*, **35,** 508–524.

BERKELHAMER, L. H. (1945), An apparatus for differential thermal analysis: *Bureau of Mines, R. I.* **3762,** 17 pages.

BRILL, OTTO (1905), Über die Dissoziation der Karbonate der Erdalkalien und des Magnesiumkarbonats: *Zeit. anorg. Chem.*, **45,** 285.

CUTHBERT, F. L., and Rowland, R. A. (1947), Differential thermal analysis of some carbonate minerals: *Am. Mineral.*, **32,** 111–116.

DANA, J. D. (1892), *A System of Mineralogy:* Sixth Edition, John Wiley & Sons, Inc., New York City.

DAVIS, W. A. (1906), Study of basic carbonates: *J. Soc. Chem. Ind.*, **25,** 788.

FAUST, GEORGE T. (1949), Differentiation of aragonite from calcite by differential thermal analysis: *Science,* **110,** no. 2859, 402–403.

FREDERICKSON, A. F. (1948), Differential thermal curve of siderite: *Am. Mineral.*, **33,** 372.

FRIEDRICH, K., AND SMITH, L. G. (1912): *Met.* vol. 9, 409. Cited in Mellor, J. W. (1927), A Comprehensive Treatise on Inorganic and Theoretical Chemistry: vol. **IV,** 353.

FRONDEL, CLIFFORD (1941), Constitution and polymorphism of the pyroaurite and sjögrenite groups: *Am. Mineral.*, **26,** 295–315.

FRONDEL, CLIFFORD (1943), Mineralogy of the oxides and carbonates of bismuth: *Am. Mineral.*, **28,** 521–540.

HEINRICH, E. WM. (1947), Beyerite from Colorado: *Am. Mineral.*, **32,** 660–669.

HURLBUT, C. S. Jr. (1946), Artinite from Luning, Nevada: *Am. Mineral.*, **31,** 365–369.

JAFFE, HOWARD W., SHERWOOD, ALEXANDER M., AND PETERSON, MAURICE J. (1948), New data on Schroeckingerite: *Am. Mineral.*, **33,** 152–157.

LARSEN, E. S., AND GONYER, F. A. (1937), Dakeite, a new uranium mineral from Wyoming: *Am. Mineral.*, **22,** 561–563.

MELLOR, J. W. (1927), A Comprehensive Treatise on Inorganic and Theoretical Chemistry: vols. **I–XVI,** Longmans, Green and Co., Ltd., London.

NOVÁČEK, RADIM (1939), The identity of dakeite and schroeckingerite: *Am. Mineral.*, **24,** 317–323.

PAVLOVITCH, STOYAN (1935), The action of heat upon some natural oxides of manganese: *Compt. Rend. Acad. Sci.*, Paris, **200,** 71–73.

SCHUMB, W. C., AND RITTNER, E. S. (1943), Polymorphism of bismuth trioxide: *J. Am. Chem. Soc.*, **65,** 1055–1060.

SILLÉN, L. G. (1938), *X*-ray Studies on bismuth trioxide: *Arkiv., Kemi., Min., Geol.*, **12A,** No. 18.

SILLÉN, L. G. (1941), On the crystal structure of monoclinic α-Bi_2O_3: *Zeit. Krist.*, **103,** 274.

ŠPLÍCHAL, J., ŠKRAMOVSKÝ, S., AND GOLL, J. (1936), Thermal decomposition of carbonate minerals: *Věda přírodní*, **17,** 206–213.